A TRIDENT SCHOLAR PROJECT REPORT

NO. 538

Evaluation of Novel Atypical β-Lactams Against Mycobacterial Ldt Enzymes Toward Combatting Antibiotic Resistance

by

Midshipman 1/C Rachel E. Sanborn, USN

UNITED STATES NAVAL ACADEMY
ANNAPOLIS, MARYLAND

USNA-1531-2

REPORT DOCUMENTATION PAGE

Form Approved
OMB No. 0704-0188

1. REPORT DATE *(DD-MM-YYYY)*	**2. REPORT TYPE**	**3. DATES COVERED** *(From - To)*
5-16-23		

4. TITLE AND SUBTITLE
Evaluation of Novel Atypical β-Lactams Against Mycobacterial Ldt Enzymes Toward Combatting Antibiotic Resistance

5a. CONTRACT NUMBER

5b. GRANT NUMBER

5c. PROGRAM ELEMENT NUMBER

6. AUTHOR(S)
Rachel E. Sanborn

5d. PROJECT NUMBER

5e. TASK NUMBER

5f. WORK UNIT NUMBER

7. PERFORMING ORGANIZATION NAME(S) AND ADDRESS(ES)

8. PERFORMING ORGANIZATION REPORT NUMBER

9. SPONSORING / MONITORING AGENCY NAME(S) AND ADDRESS(ES)
U.S. Naval Academy
Annapolis, MD 21402

10. SPONSOR/MONITOR'S ACRONYM(S)

11. SPONSOR/MONITOR'S REPORT NUMBER(S)
Trident Scholar Report no. 538 (2023)

12. DISTRIBUTION / AVAILABILITY STATEMENT

This document has been approved for public release; its distribution is UNLIMITED.

13. SUPPLEMENTARY NOTES

14. ABSTRACT

Antimicrobial resistance continues to grow as a global issue. This work aims to combat this concern by investigating L,D-transpeptidase (Ldt) enzymes as potential new drug targets using atypically modified β-lactam compounds. Ldts perform an essential function in formation of the peptidoglycan layer of mycobacterial cell walls. These unique Ldt enzymes provide an avenue of drug design by exploiting their essentiality in mycobacterial cell wall biosynthesis and nature specific to mycobacterial infections.

There are six evolutionarily distinct classes of mycobacterial Ldts and different mycobacteria species may have all or varying numbers of Ldt classes present. Class 2 Ldts from various mycobacterial species—including that which causes tuberculosis—were the target in this study and were inactivated by both a commercial and synthetic carbapenem, imipenem and compound 10a respectively. Compound 10a is an atypically modified carbapenem, a subclass of β-lactam, with demonstrated promise as a potential treatment.

The two carbapenems of interest were evaluated based on their acylation kinetic profiles generated via stopped-flow tryptophan fluorescence and DynaFit non-linear regression software. Mass spectrometry data supported the nonlinear fits and rate constants produced by DynaFit software. Investigating the acylation kinetics of these compounds will further guide drug design studies toward identifying new Ldt inhibitors.

15. SUBJECT TERMS
Enzyme kinetics, Stopped-flow, L,D-transpeptidase, Mycobacterium tuberculosis, Non-tuberculous mycobacteria (NTM)

16. SECURITY CLASSIFICATION OF:			**17. LIMITATION OF ABSTRACT**	**18. NUMBER OF PAGES**	**19a. NAME OF RESPONSIBLE PERSON**
a. REPORT	**b. ABSTRACT**	**c. THIS PAGE**		18	**19b. TELEPHONE NUMBER** *(include area code)*

U.S.N.A. --- Trident Scholar project report; no. 538 (2023)

EVALUATION OF NOVEL ATYPICAL β -LACTAMS AGAINST MYCOBACTERIAL LDT ENZYMES TOWARD COMBATTING ANTIBIOTIC RESISTANCE

by

Midshipman 1/C Rachel E. Sanborn
United States Naval Academy
Annapolis, Maryland

Certification of Adviser Approval

Associate Professor Leighanne A. Basta
Chemistry Department

Acceptance for the Trident Scholar Committee

Professor Maria J. Schroeder
Associate Director of Midshipman Research

USNA-1531-2

Abstract

Antimicrobial resistance continues to grow as a global issue. This work aims to combat this growing concern by investigating L,D-transpeptidase (Ldt) enzymes as potential new drug targets using atypically modified β-lactam compounds. Ldts perform an essential function in the formation of the peptidoglycan layer of mycobacterial cell walls. These unique Ldt enzymes provide an avenue of drug design by exploiting their essentiality in mycobacterial cell wall biosynthesis and nature specific to mycobacterial infections.

There are six evolutionarily distinct classes of mycobacterial Ldts and different mycobacteria species may have all or varying numbers of Ldt classes present. Class 2 Ldts are the most well studied due to their predominance in literature. Class 2 Ldts from various mycobacterial species—including that which causes tuberculosis—were inactivated by both a commercial and synthetic carbapenem, imipenem and compound **10a** respectively. Compound **10a** is an atypically modified carbapenem, a subclass of β-lactam, with demonstrated promise as a potential treatment since it more effectively killed both *Mycobacterium tuberculosis* (*Mtb*) and *Mycobacterium abscessus* (*Mab*) than a commercial carbapenem *in vitro*.

The two carbapenems of interest were evaluated based on their acylation kinetic profiles generated via stopped-flow tryptophan fluorescence and DynaFit non-linear regression software. Mass spectrometry data supported the nonlinear fits and rate constants produced by DynaFit software and aided in monitoring the conformational changes that occurred during inactivation, thus elucidating the mechanism by which inactivation occurs. Investigating the acylation kinetics of these compounds will further guide drug design studies toward identifying new Ldt inhibitors. Ldt-specific inhibitors would minimize undesirable gastrointestinal side-effects that are often attributed to long term antibiotic use by avoiding interaction with enzymes that are active in other biochemical processes.

KEYWORDS: enzyme kinetics, stopped-flow, L,D-transpeptidase, *Mycobacterium tuberculosis,* non-tuberculous mycobacteria (NTM)

Table of Contents

Acknowledgement

We gratefully acknowledge Dr. John Buynak for providing atypical carbapenem **10a**, and Dr. Kyle Rohde for supplying our lab with the *ldt*$_{Mab2}$/pET28b plasmid. Finally, we thank Dr. Phil Mortimer at Johns Hopkins University for collecting UPLC-MS data.

Background and Previous Work

Tuberculosis (TB) is caused by *Mycobacterium tuberculosis* (*Mtb*) and is currently the second leading cause of death by infectious disease in the world—and the first before the COVID-19 pandemic began[1]. Even drug-susceptible *Mtb* infections require 6 months of treatment with multiple drugs, and the rise of drug-resistant *Mtb* is becoming an increasingly dire public health issue. By 2050, the World Health Organization predicts that deaths attributable to antimicrobial resistant infections will surpass cancer as a leading cause of death[2]. Thus, there is a critical need for new antibiotics.

All mycobacterial cell walls, including the cell walls of *Mtb*, have a distinctive peptidoglycan (PG) layer that is essential to the cell's survival. The PG layer forms a mesh-like structure around the cell membrane, providing shape and rigidity (Figure 1). This layer also allows the cell to withstand osmotic pressure differences across the mycobacterial cell membrane. Without properly organized and crosslinked PG, the cells cannot survive.

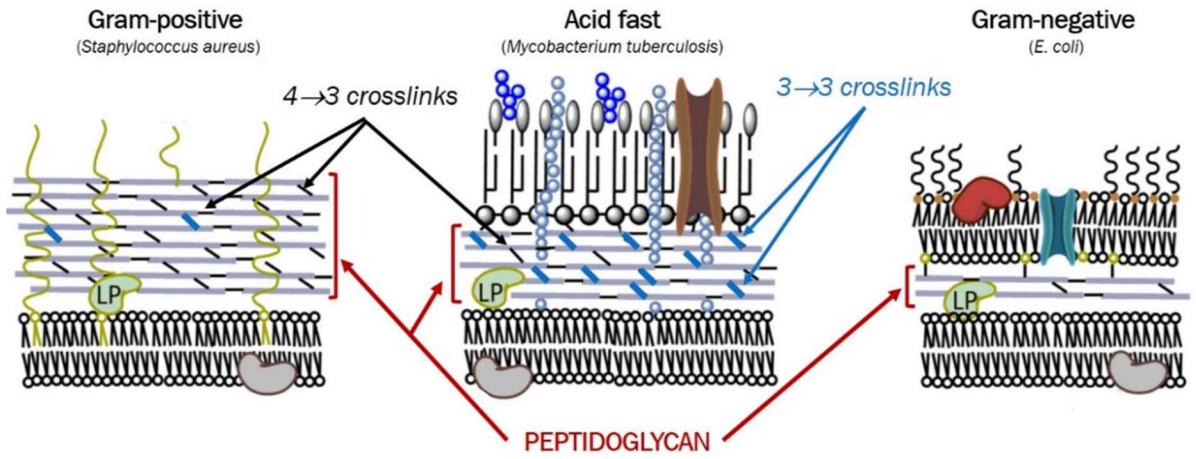

Figure 1. *Nearly all bacteria possess a peptidoglycan (PG) layer that is either predominantly 4→3 (black bars) or 3→3 crosslinked (blue bars). Acid-fast bacteria like mycobacteria have predominantly 3→3 crosslinked PG. Without properly crosslinked PG, the cell cannot survive*[3].

PG components are comprised of chains of amino acids, and in most bacteria, like *Escherichia coli*, the PG layer is primarily crosslinked between the 4th and 3rd amino acids, thereby earning the name of a 4→3 crosslink (Figure 1). The enzymes which form these 4→3 cross linkages are called penicillin-binding proteins (PBPs). PBPs are the targets of β-lactam antibiotics which include penicillin and amoxicillin (Figure 2).

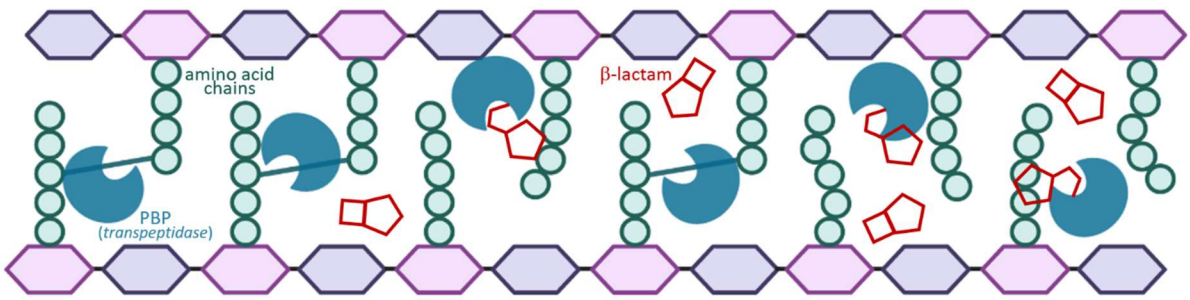

Figure 2. *β-Lactam antibiotics (like penicillin) inhibit PBPs and prevent the formation of PG crosslinks, resulting in a destabilized cell wall.*

Significantly, 60% of all clinically administered antibiotics are β-lactams, highlighting the essentiality of PG crosslinking and these 4→3 crosslinks in bacteria. However, the PG layer of mycobacteria is unique. The PG of mycobacterial species, including that of *Mtb*, is mainly 3→3 crosslinked (Figures 1 and 3), not 4→3 crosslinks like most other bacteria. These crosslinks are formed by different enzymes called L,D-transpeptidases (Ldts). Ldts and PBPs are different in structure and are not targeted by the same drugs. Typical β-lactam antibiotics—which target PBPs—are largely ineffective against mycobacterial infections because they are targeting the wrong enzymes. This, in part, explains why mycobacterial infections have not been historically treated with β-lactam antibiotics.

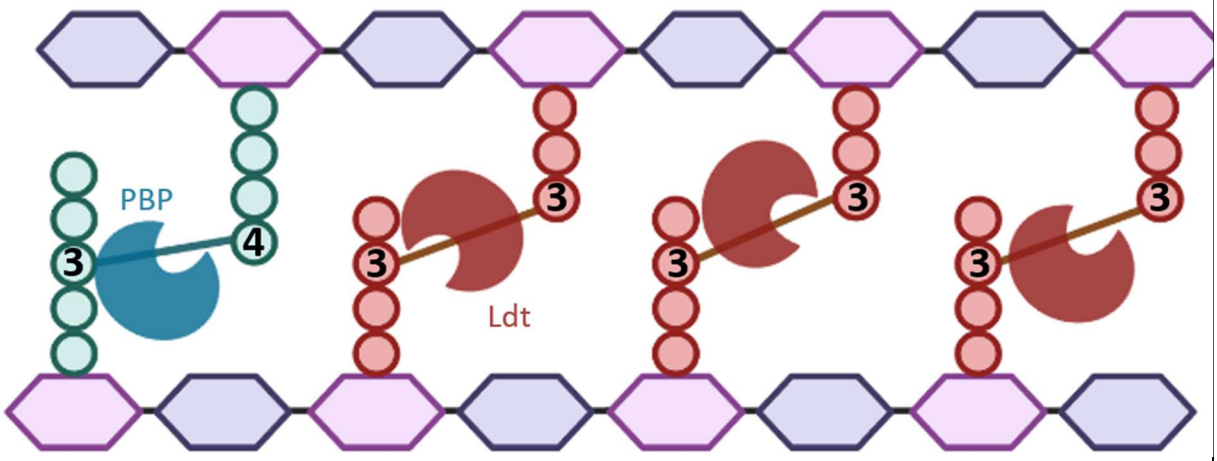

Figure 3. The *PG layer of mycobacterial species is ~80% 3→3 crosslinked.*

There are six evolutionarily distinct classes of mycobacterial Ldts and different mycobacteria species may have all or varying numbers of Ldt classes present[4]. The exact roles these Ldts play in the proper maintenance of mycobacterial PG is not entirely understood. Studies have pointed to the class 2 Ldt from *Mtb*, Ldt_{Mt2}, as the 'dominant' Ldt, because Ldt_{Mt2} expression levels are ~5-fold higher than the other *Mtb* Ldts. Further, *Mtb* lacking a functional copy of Ldt_{Mt2} are less virulent, have observable morphological defects in culture, and are more susceptible to antibiotics[5].

Class 2 Ldts have been the focus of most mycobacterial enzyme literature following this identification as the "dominant" enzyme in *Mtb*. By extension, the class 2 Ldt enzyme from *M. smegmatis* (*Msm*), *M. abscessus* (*Mab*), and *M. chelonae* (Mab) were also selected for comparison in this study. *Mab* is an opportunistic pathogen that commonly infects the lung tissue of immunocompromised patients and is particularly problematic for cystic fibrosis patients. *Mch* is closely related to *Mab* which makes it particularly interesting for a comparison study. Finally, *Msm* is a model organism for *Mtb* study[6]. Each of these mycobacterial species are unique, and while closely related from an evolutionary perspective, their Ldt enzymes may have different activities. Thus, studying the mechanisms of Ldt inactivation by different drugs will inform future drug design on targeting Ldt enzymes in various mycobacterial infections.

An infection is considered cured when the bacteria causing it has been killed. The most effective antibiotics target essential bacterial cellular processes, like the formation of the PG layer. If Ldt enzymes are inhibited, the mycobacterial PG cannot be properly 3→3 crosslinked, which ultimately causes cell death, thereby clearing the infection. Current drugs that are effective at inhibiting Ldt function are carbapenems, a subclass of β-lactams (not to be confused with the β-lactam class as a whole, members of which are largely ineffective against Ldt enzymes). Figure 4 provides a few examples of β-lactam derivatives including carbapenems.

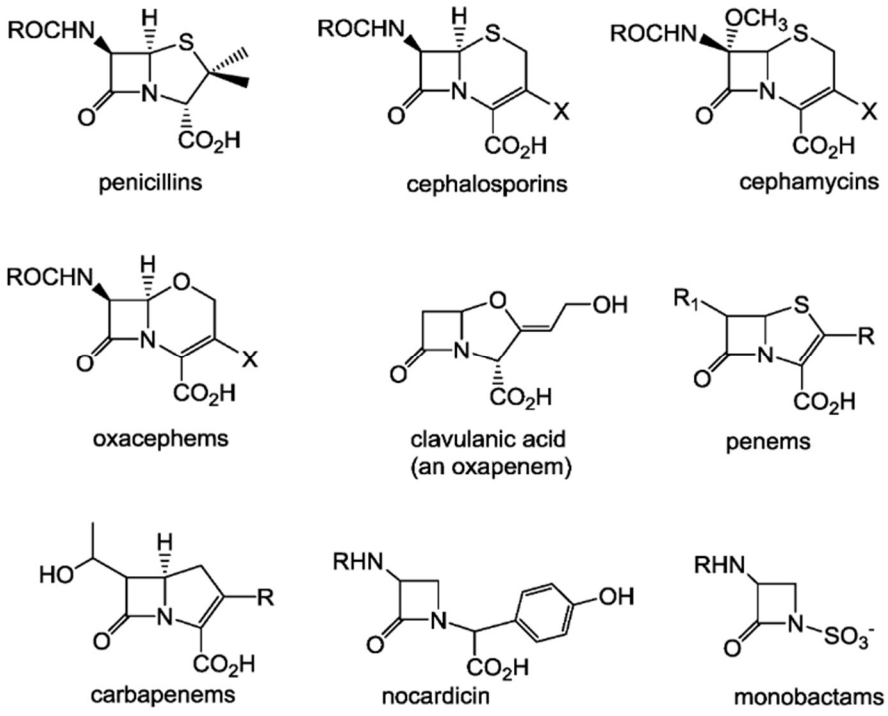

Figure 4. *Examples of β-lactam derivatives including the subclass of carbapenems (bottom left)*[7].

Literature indicates that inhibition of Ldts by carbapenems occurs via a two-step mechanism (Figure 5)[8]. The first step generates a negatively charged anionic amine enzyme-drug complex

(ED^{An}). The ED^{An} is then protonated, thereby forming the fully inactivated ED^{Ac} complex. This inhibited ED complex can no longer form the 3→3 crosslinks in mycobacterial PG.

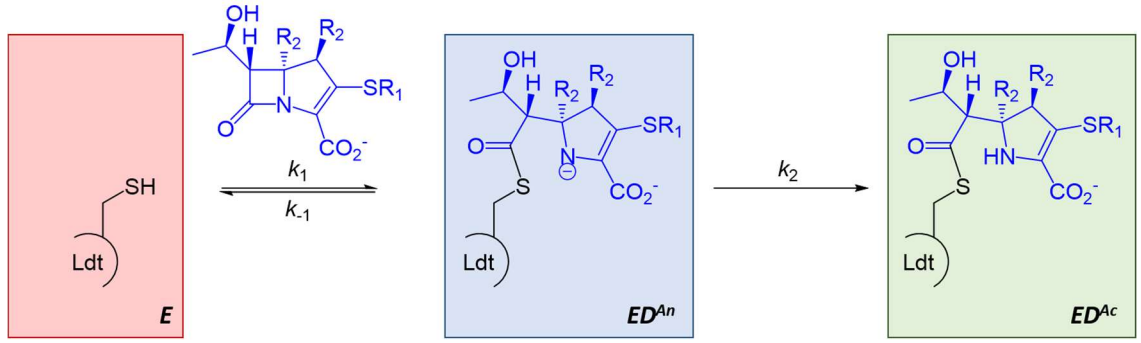

Figure 5. *Two step mechanism of Ldt inactivation by a carbapenem demonstrating reversibility of the first step[8]. R_1 = C2 modifications; R_2 = methyl group or hydrogen atom.*

Imipenem is a commercially available carbapenem β-lactam antibiotics that inhibits Ldt function, and is currently one of a combination of drugs in use for combatting *Mab* pulmonary disease[9]. Imipenem was used as the commercial carbapenem to which our novel atypical β-lactam, compound **10a**, was compared. Dr. John Buynak (Southern Methodist University) is a synthetic chemist that specializes in making β-lactams. He synthesizes atypical β-lactam compounds, and he and Dr. Basta are working toward creating a mycobacteria-specific drug that is more effective than the current commercial drugs in use. Historically, chemists have made modifications to β-lactams at the 2nd carbon (labeled 2 on Figure 6, referred to as C2), because the C2 position is the most receptive to synthetic modification. His compounds, however, are considered "atypical" because he alters the β-lactams at the 5th carbon (labeled 5 on Figure 6, referred to as C5)[10].

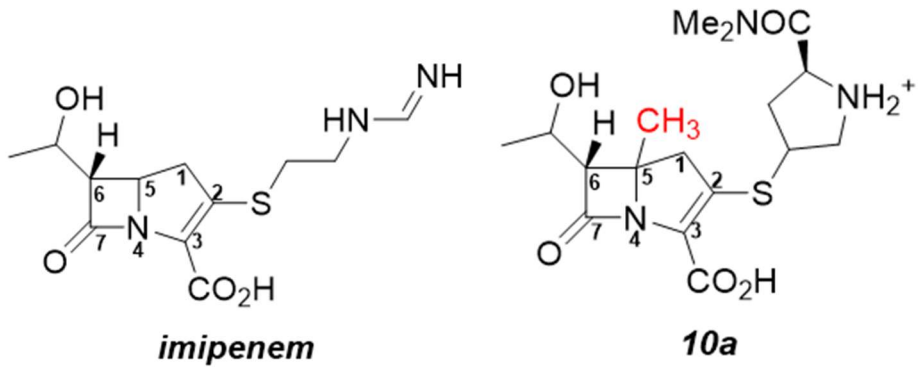

Figure 6. *Imipenem belongs to the β-lactam subclass of carbapenems. Compound **10a** is a synthetic 'atypical' carbapenems with modifications at the C5 position.*

Compound **10a** shows significant promise as a potential treatment of mycobacterial infections as demonstrated in a 2021 study published by Dr. Basta and her collaborators[11]; compound **10a** inhibits Ldt_{Mt2} and more effectively kills *Mtb* and *Mab* than meropenem, another commercial carbapenem, *in vitro*. Synthetic **10a** has lower minimum inhibitory concentration (MIC) values

than commercial meropenem against *Mtb*, meaning less **10a** is needed in order to kill these mycobacteria. This 2021 study also evaluated other atypically modified carbapenems, compounds **10b**, **13a**, and **13b**, however, **10a** performed the best and was therefore selected for subsequent investigations.

	Mtb		*Mab*	
carbapenem	alone	with clavulanate (5 μg/mL)	alone	with avibactam[#] (5 μg/mL)
meropenem*	1.1	0.5	2.6	3.1
10a	0.1	0.1	0.4	0.5
10b	2.1	1.6	22.3	11.6
13a	0.8	0.6	7.5	5.8
13b	7.9	5.6	NA	NA

[a]NA: No activity at the highest conc. (30.3 μg/mL). *$P < 0.05$, comparison of +/- clavulanate. [#]No statistical difference with +/- avibactam.

Table 1. *MIC values (⌈g/mL) of C5⟨-substituted carbapenem antibiotics against Mtb and Mab*[11].

Mycobacteria express β-lactamase enzymes that degrade β-lactam antibiotics, which is an additional reason that β-lactams have historically not been used to treat *Mtb*[12]. Consequently, when MIC studies look at the effects of β-lactams on *Mtb* killing, β-lactamase inhibitors, like clavulanate and avibactam, are co-administered. Significantly, **10a** has comparable MIC values in the presence *and* absence of the β-lactamase inhibitors (Table 1), indicating **10a** is resistant to degradation by β-lactamases. Conversely, the MIC of meropenem decreases from 1.1 ⌈g/mL to 0.5 ⌈g/mL indicating more meropenem is required to kill *Mtb* in the absence of clavulanate.

The study presented here expands upon the observations that **10a** is a β-lactamase-stable Ldt_{Mt2} inhibitor and has low MIC values against pathogenic *Mtb* and *Mab*. Here, we evaluate the inhibition of multiple class 2 Ldt enzymes including Ldt_{Mt2} and the class 2 Ldt of *Mab*, Ldt_{Mab2}, by both this synthetic carbapenem, and a commercially available carbapenem currently in use as a medical treatment. We also investigate inactivation of *Msm* LdtB and *Mch* Ldt_{Mch2} by these carbapenems toward determining whether the inactivation mechanism of class 2 Ldts is universal.

Materials and Methods

Data was collected via stopped-flow tryptophan fluorescence and ultraperformance liquid chromatography high resolution mass spectrometry (UPLC-HRMS). Atypical carbapenem **10a** was supplied by Dr. John Buynak at Southern Methodist University. All other materials were purchased from commercial sources.

Purification of Ldt_{Mt2}. Soluble Ldt_{Mt2} was produced in *Escherichia coli* and purified by affinity chromatography as described previously[13]. Briefly, *E. coli* BL21(DE3) cells harboring a plasmid that expresses a truncated version of Ldt_{Mt2} ($\Delta^{1\text{-}26}ldt_{Mt2}$-pET28b) were grown in LB broth to an OD_{600} of ~0.5 at 37 °C with shaking. Protein overexpression was induced with 100 μM isopropyl 1-thio-β-D-galactopyranoside (IPTG), and following induction, cells were incubated with shaking at 20 °C for an additional 14−20 h. Cells were harvested at 4 °C, resuspended in protein purification

buffer (25 mM Tris, pH 8.0, 400 mM NaCl, and 10% glycerol), and lysed by ultrasonication. Cell debris was removed by centrifugation (15,000 rpm, 30 min) at 4 °C. The supernatants were passed over a washed nickel-nitrilotriacetic acid (Ni-NTA) resin at room temperature, and His_6-tagged Ldt_{Mt2} was eluted in ice-cold protein purification buffer containing imidazole. Fractions containing Ldt_{Mt2} (as determined by SDS-PAGE) were combined, and protein concentration was determined using the Bio-Rad Protein Assay with bovine serum albumin (BSA) as a standard. Samples were dialyzed overnight at 4 °C against 50 mM Tris, pH 8.0, 100 mM NaCl, and 10% glycerol. The proteins were subjected to a second dialysis against 50 mM Tris, pH 8.0, 100 mM NaCl, 10% glycerol, and 1 mM tris(2-carboxyethyl)phosphine (TCEP). The protein concentration was determined using the calculated Molar extinction coefficient of 71,390 $M^{-1}cm^{-1}$. Purified Ldt_{Mt2} was flash frozen in liquid N_2 and stored long-term at −80 °C.

Mass spectrometry. Ldt_{Mt2} (10 μM) was incubated in the presence or absence of 200 μM carbapenem in 100 mM phosphate buffer, pH 6 for two minutes at 10 °C. Samples were quenched with trifluoroacetic acid (final concentration 0.1% v/v) and analyzed by UPLC-HRMS.

Spectrofluorimetry. Kinetic experiments were performed in 100 mM phosphate buffer, pH 6.0 at 10 °C. The final concentrations of Ldt_{Mt2} and drug were 5 μM and 50 or 200 μM, respectively. Excitation was performed at 224 nm with a 5 nm slit width. (Note that excitation was performed at 224 nm so as to not interfere with opening of the β-lactam rings as previously described[8].) Emission was determined at 335 nm with a 5 nm slit width (Ldt_{Mt2}, Ldt_{Mab2}, Ldt_{Mch2}) or 2.5 nm (LdtB). The fluorimeter photomultiplier was set to 600 V (Ldt_{Mt2}, Ldt_{Mab2}, Ldt_{Mch2}) or 700 V (LdtB), and experiments were performed a minimum of three times.

Kinetic analyses. All spectra were corrected by subtracting emission spectra acquired on samples containing no drug, and were additionally then normalized in GraphPad Prism by taking each individual sample emission spectrum and defining the maximum value and minimum value of the spectra as 1 and 0, respectively. Several mechanisms were examined using the global non-linear regression analysis software DynaFit[14], and all data collected for both the 50 μM and 200 μM carbapenem concentrations were fit simultaneously. Each fit generated a rate constant for each step of the proposed mechanism as well as a 95% confidence interval for the respective rate constant. If a fit generated a rate constant that fell within an open-ended 95% confidence interval (as was the case with **10a** and Ldt_{Mab2}, Ldt_{Mch2}, LdtB), the Monte-Carlo method for confidence intervals was utilized to determine suitability of the fit.

Results and Discussion

Determining the mechanisms of Ldt inactivation. Three mechanisms of Ldt inhibition were considered [equations 1-3]. The previously reported mechanism of carbapenem inhibition [equation 2] was rejected due to the non-appreciable amount of reversibility in the first step as determined by our experimental data[8]. The rate constant k_{-1}, which measures the breakdown of ED^{An} back to E + D, is essentially zero for all drug and enzyme combinations. Similarly, reversibility in the second step was also considered and rejected for the same reasons [equation 3].

$$E + D \rightarrow ED^{An} \rightarrow ED^{Ac} \qquad [1]$$

$$E + D \leftrightarrow ED^{An} \rightarrow ED^{Ac} \quad [2]$$

$$E + D \rightarrow ED^{An} \leftrightarrow ED^{Ac} \quad [3]$$

Therefore, all reactions were found to fit the two-step mechanism proposed in Figure 7, since no appreciable amount of reversibility was observed in either step.

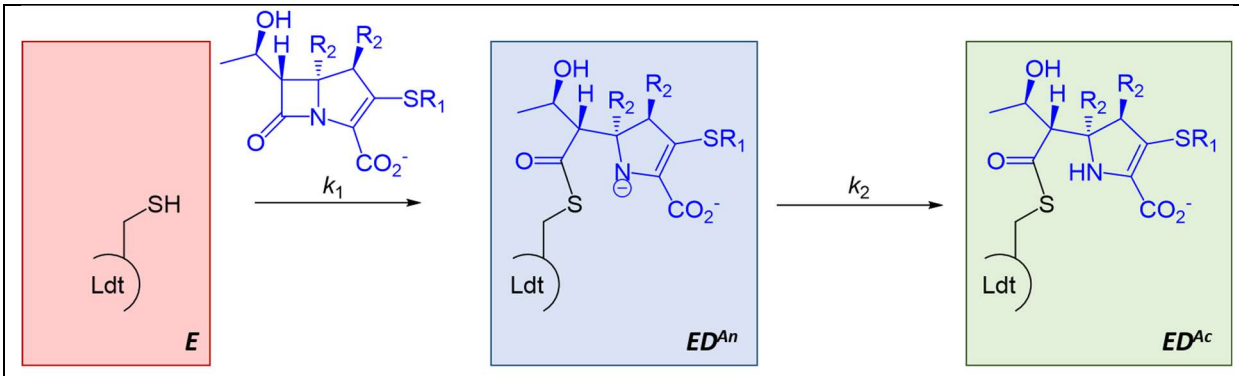

***Figure** 7. The class 2 Ldts evaluated in this study all follow a two-step mechanism, where there is no appreciable reversibility contributing to the kinetic rate constants.*

Determining the kinetic parameters of Ldt inactivation by imipenem. The following graphs display the collected spectra and lines of best fit for reactions with imipenem and the four class 2 Ldt enzymes of interest (Figure 8). Each colored line represents the best fit for a single data set, of which many are overlaid within each graph. Compiling the data in this manner allows the software to generate fits based on the data collected in replicate as opposed to each spectrum analyzed individually which would be more susceptible to random error.

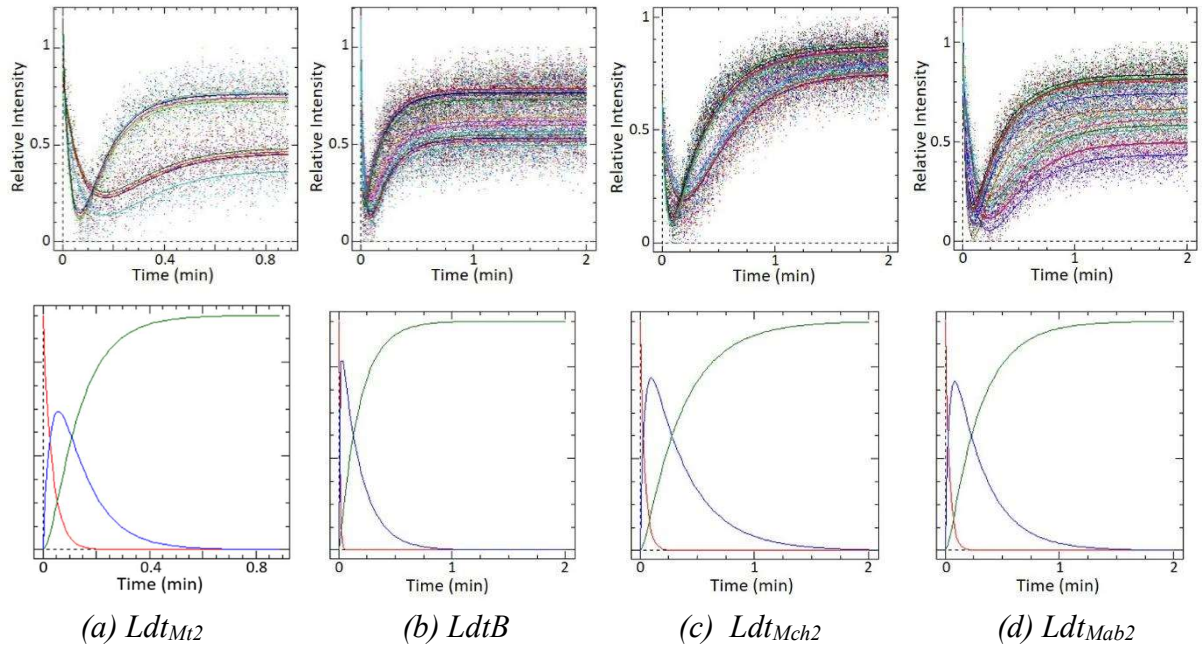

Figure 8. *Stopped-flow tryptophan fluorescence data and lines of best fit for Ldt inactivation by imipenem (top panels) and reaction progress (bottom panels). For the reaction E + D □ ED^{An} □ ED^{Ac}, where E is red, ED^{An} is blue, and ED^{Ac} is green.*

Each graph has two distinct groupings of best fit lines (50 and 200 μM). The higher the drug concentration, the faster, and often stronger, the quench in signal which causes the distinction seen above. DynaFit software accounts for the concentration of both enzyme and drug in the reaction in order to generate rate constants.

Additional graphical output collected from the DynaFit software includes the changes in molecular species over the course of the reaction (Figure 8). At the start of the reaction (t = 0 minutes), the only present species is free enzyme, E. As seen with all of the Ldts examined, free enzyme is rapidly depleted as the enzyme-drug anion intermediate complex, ED^{An} forms, and then ED^{An} concentrations fall as it is converted into the final enzyme-drug acylated complex, ED^{Ac}, during the second step of the reaction. The following generated output confirms that the expected reaction is not only occurring, but is being used to fit the spectra and produce the rate constants. The rate constants for inactivation of the class 2 Ldts by imipenem are shown in Table 2. In all cases, initial acylation is rate limiting (k_1), and protonation of the ED^{An} species to ED^{Ac} is rapid (faster k_2).

	***Mtb* Ldt_{Mt2}**	***Msm* LdtB**	***Mch* Ldt_{Mch2}**	***Mab* Ldt_{Mab2}**
k_1 ($M^{-1}\cdot min^{-1}$)	0.1478 ± 0.0032	0.568 ± 0.012	0.1279 ± 0.0022	0.1431 ± 0.0016
k_2 (min^{-1})	9.14 ± 0.917	5.729 ± 0.063	2.91 ± 0.025	3.602 ± 0.029

Table 2. Inactivation of class 2 Ldts by imipenem.

*Determining the kinetic parameters of Ldt inactivation by **10a***. Ldt inactivation by **10a** not only yielded unique spectra relative to those observed with imipenem, but also among the four Ldts examined (Figure 9). For example, in the case of imipenem, ED^{An} forms rapidly on all Ldts, and concentrations of free enzyme drop to zero after 15 seconds (Figure 8). However, free enzyme persists in the presence of **10a** for as long as 60 seconds in some cases (Figure 9). Further, the rates of ED^{An} and ED^{Ac} formation are markedly different among paralogous Ldts (*i.e.* Ldt_{Mt2} vs Ldt_{Mab2}, Table 3).

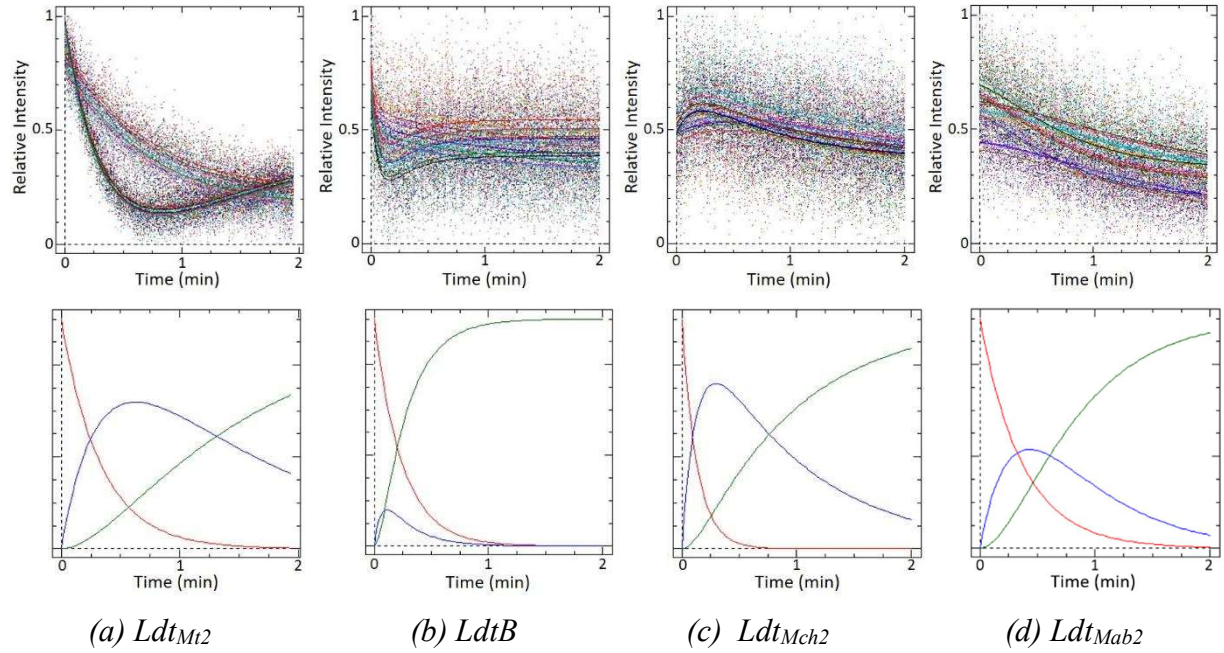

Figure 9. *Stopped-flow tryptophan fluorescence data and lines of best fit for Ldt inactivation by **10a** (top panels) and reaction progress (bottom panels). For the reaction E + D □ ED^{An} □ ED^{Ac}, where E is red, ED^{An} is blue, and ED^{An} is green.*

	Mtb **Ldt_{Mt2}**	***Msm*** **LdtB**	***Mch*** **Ldt_{Mch2}**	***Mab*** **Ldt_{Mab2}**
k_1 ($\lceil M^{-1}\cdot min^{-1}$)	0.0152 ± 0.0002	0.0209 ± 0.0017	0.0387 ± 0.0041	0.0137 ± 0.0007
k_2 (min^{-1})	0.711 ± 0.066	16.3 ± 1.2	1.11 ± 0.13	1.94 ± 0.18

Table 3. Inactivation of class 2 Ldts by **10a**.

These findings highlight the differences between the various class 2 Ldts. No two outputs are exactly the same, therefore there are unique interactions in each combination of enzyme and drug.

Generally, imipenem more rapidly acylates class 2 Ldts than **10a** (Tables 2-3). However, there are notable differences; most strikingly, the rate of protonation of the **10a** anionic intermediate on LdtB is ~8-20 times faster than the same step with the other Ldts (Table 3). Rapid protonation of the **10a** ED^{An} complex to form ED^{Ac} on LdtB is further supported by the mechanism. As indicated

in Figure 10b, ED^{An} does not accumulate to appreciable amounts in comparison to the Ldts examined and is rapidly converted to ED^{Ac}. Taken together, these data demonstrate that class 2 Ldts are differentially acylated by both imipenem and **10a**.

Statistical analysis to confirm the mechanisms of inactivation. The confidence intervals of each generated rate constant were also considered to ensure suitability of fit. All reactions with imipenem had rate constants within the 95% confidence interval, as did Ldt_{Mt2} and **10a**. The rate constants initially generated in reactions with LdtB, Ldt_{Mch2}, Ldt_{Mab2} and **10a** did not fall within their respective 95% confidence intervals (Figure 10); however, this is often the case with bimolecular reactions[15].

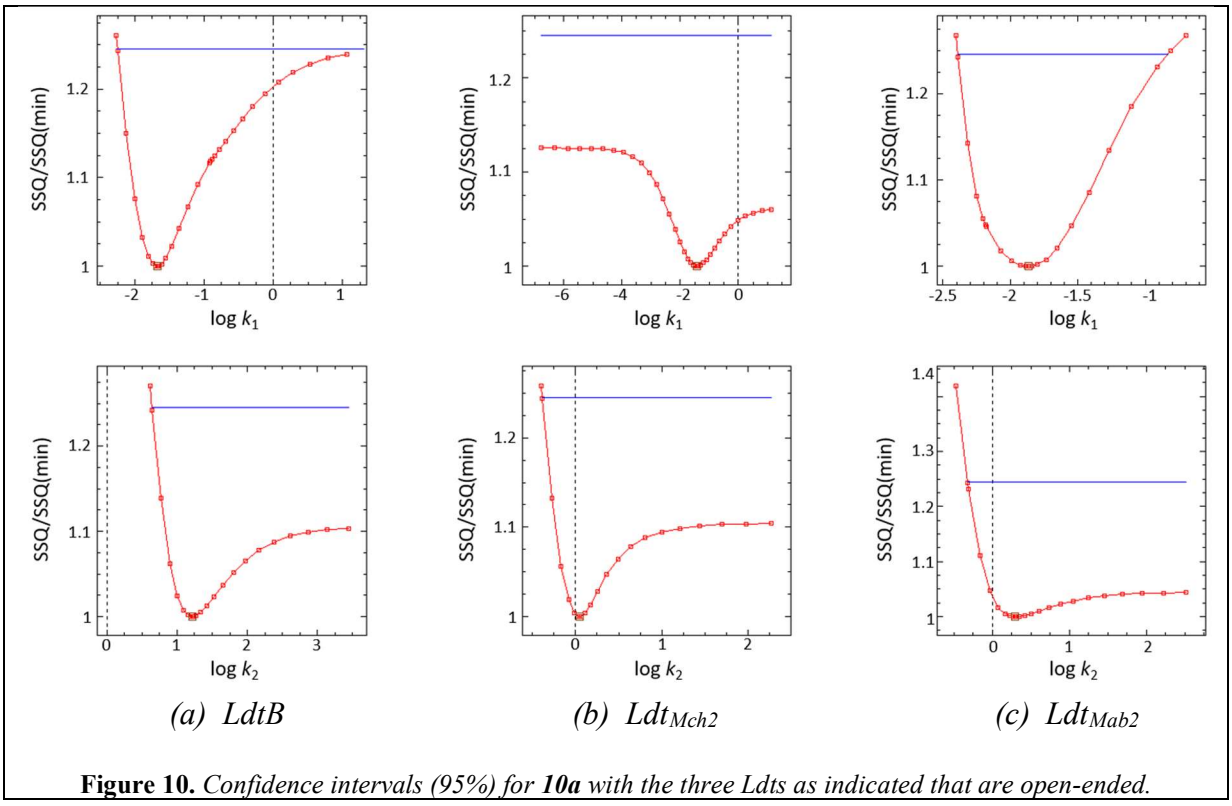

Figure 10. *Confidence intervals (95%) for **10a** with the three Ldts as indicated that are open-ended.*

In order to ensure the accuracy of our models, we employed the Monte-Carlo method as a secondary check of suitability (Figure 11) using DynaFit. When the Monte-Carlo method is employed in DynaFit, 1000 data sets are created based off of the original collected data. Each new data set has different and unique random errors introduced in order to gather the scope of variability in a given data set. Thus, when analyzed, each data set will have a slightly different rate constant generated from the unique data set and the amount of times a given rate constant appears from the 1000 is represented in the histogram graphs. The more frequently a number is generated, the more likely it is to be the best fit, and the two rate constants are plotted on a correlation plot to provide the upper and lower limits of possibilities.

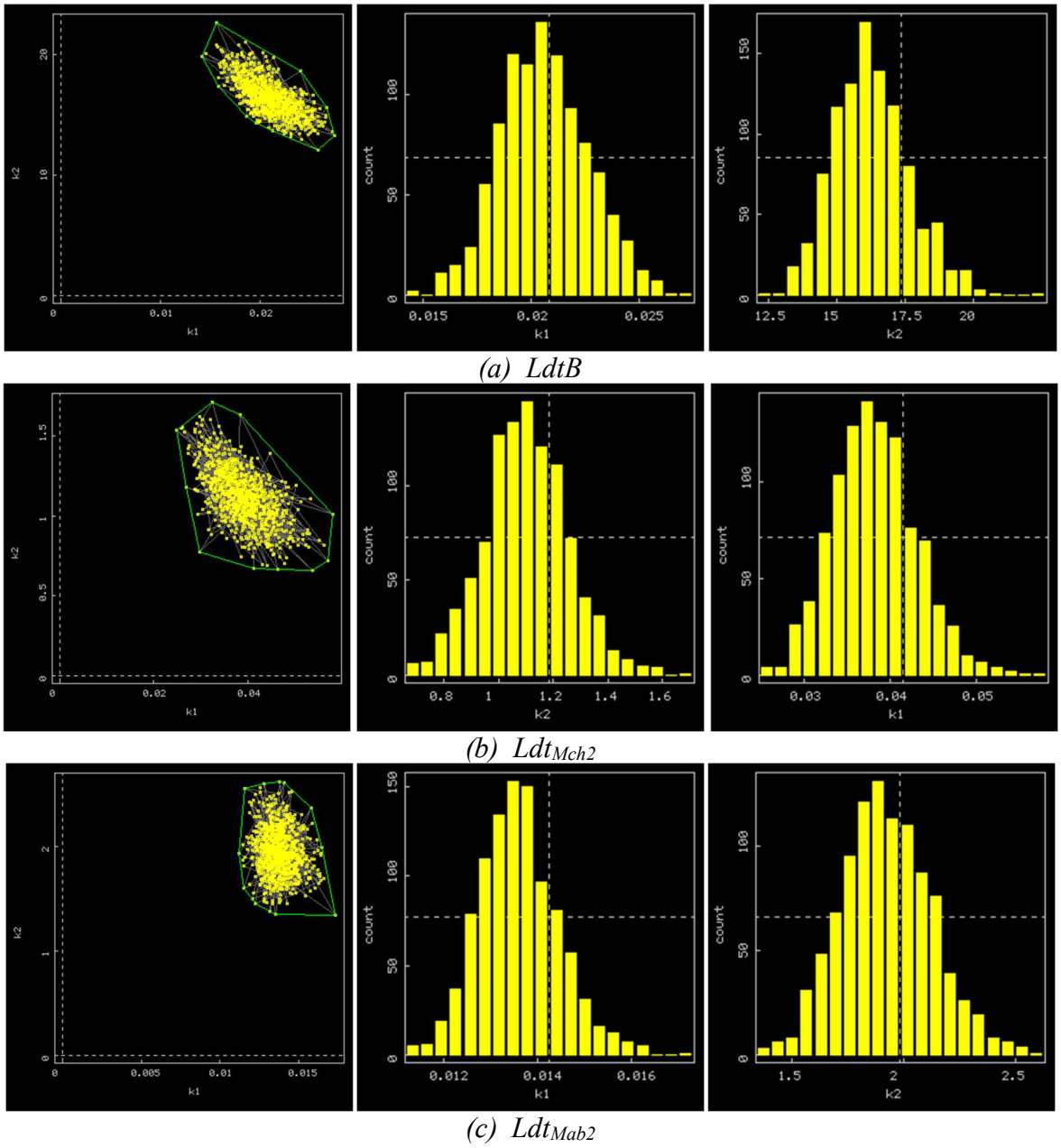

Figure 11. *Monte-Carlo method correlation plots (left column) and histograms indicating the number of occurrences of a given rate constant (k_1 or k_2).*

For each Ldt, these histograms are centered around the rate constants generated from the earlier lines of best fit (Table 3), confirming that our data accurately reflect the true rate constants.

Confirming formation of Ldt adducts by mass spectrometry. Mass spectrometry data further support the finding of differential acylation patterns of Ldt_{Mt2} with imipenem and **10a** (Figure 12). Our mass spectrometry data support our mechanism and indicate that Ldt_{Mt2} is completely acylated by imipenem within 10 seconds while free enzyme is still detected in the **10a** reaction after ~30 seconds. Consequently, this supports the slower rate constants associated with **10a** compared to those of imipenem.

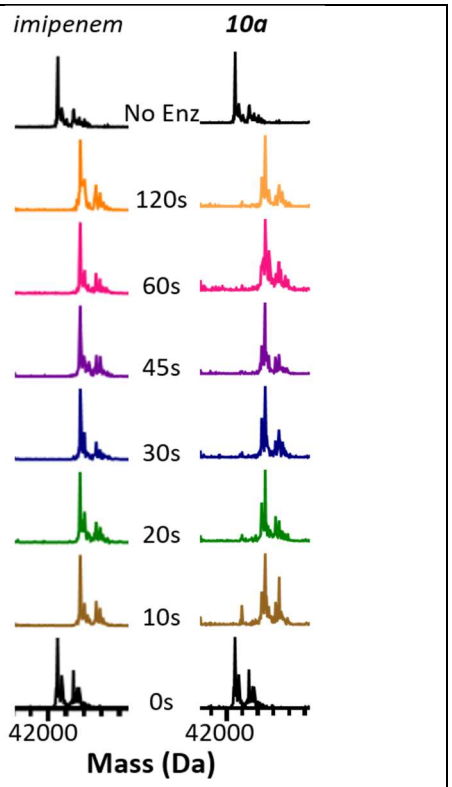

Figure 12. *High resolution mass spectrometry data of Ldt_{Mt2} with imipenem and **10a**.*

Conclusions

Imipenem inhibits Ldt_{Mt2}, LdtB, Ldt_{Mch2}, and Ldt_{Mab2} faster than **10a**. This is supported by both the stopped-flow tryptophan fluorescence kinetic data as well as the mass spectrometry data. Additionally, both the commercial and synthetic carbapenem follow the same two-step mechanism of inactivation [equation 1]. Therefore, despite the atypical C5 alteration, **10a** is still capable of reacting with the catalytic cysteine residue in the active site of Ldt enzymes. However, the class 2 Ldt enzymes are differentially acylated both across drugs and across mycobacterial species. No two Ldts behaved the same, indicating that unique interactions occur between each enzyme and drug pairing.

Ldt_{Mch2} and Ldt_{Mab2} have the most similar kinetic profiles out of the four Ldts studied, which is not surprising given their similarity in structure; *Mab* and *Mch* share the most recent ancestor and, as a result, have enzymes with the most similar active site environments. Further evidence for

differential acylation may be linked to other active site differences, but specific connections are beyond the scope of this work.

The findings of this study are of particular importance for guiding future drug design because they highlight the Ldt enzymatic behaviors unique to mycobacterial species. Despite targeting the same enzyme in each mycobacterial species, the rates of reaction demonstrate distinctive kinetic profiles, indicating that one drug may not be a viable solution for all mycobacterial infections.

Additionally, the differences in activity between the two carbapenems with respect to a single Ldt is also important in informing drug design, specifically with consideration to alternate modifications. While the **10a** with a C5 alteration is still reactive, it was not as reactive as imipenem which does not have a substituent at the C5 position. Other potential alterations could lead to improved kinetic activity against class 2 Ldts with our work as precedence that these atypical modifications can still follow the mechanism proposed in literature.

References

1. Tuberculosis. *World Health Organization* 2022 Oct 27. https://www.who.int/news-room/fact-sheets/detail/tuberculosis (accessed on 2023-04-17).
2. New report calls for urgent action to avert antimicrobial resistance crisis. *World Health Organization.* 2019 Apr 29. https://www.who.int/news/item/29-04-2019-new-report-calls-for-urgent-action-to-avert-antimicrobial-resistance-crisis (accessed on 2022-01-11).
3. Maitra A, Munshi T, Healy J, Martin LT, Vollmer W, Keep NH, Bhakta S. Cell wall peptidoglycan in Mycobacterium tuberculosis: An Achilles' heel for the TB-causing pathogen. FEMS Microbiol Rev. 2019 Sep 1;43(5):548-575. doi: 10.1093/femsre/fuz016. PMID: 31183501; PMCID: PMC6736417.
4. Sanders AN, Wright LF, Pavelka MS. Genetic characterization of mycobacterial L,D-transpeptidases. Microbiology (Reading). 2014 Aug;160(Pt 8):1795-1806. doi: 10.1099/mic.0.078980-0. Epub 2014 May 21. PMID: 24855140; PMCID: PMC4117223.
5. Gupta R, Lavollay M, Mainardi JL, Arthur M, Bishai WR, Lamichhane G. The Mycobacterium tuberculosis protein LdtMt2 is a nonclassical transpeptidase required for virulence and resistance to amoxicillin. Nat Med. 2010 Apr;16(4):466-9. doi: 10.1038/nm.2120. Epub 2010 Mar 21. PMID: 20305661; PMCID: PMC2851841.
6. Shiloh MU, Champion PA. To catch a killer. What can mycobacterial models teach us about Mycobacterium tuberculosis pathogenesis? Curr Opin Microbiol. 2010 Feb;13(1):86-92. doi: 10.1016/j.mib.2009.11.006. Epub 2009 Dec 23. PMID: 20036184; PMCID: PMC2876343.
7. Konaklieva MI. Molecular Targets of β-Lactam-Based Antimicrobials: Beyond the Usual Suspects. *Antibiotics*. 2014; 3(2):128-142. https://doi.org/10.3390/antibiotics3020128
8. Triboulet S, Edoo Z, Compain F, Ourghanlian C, Dupuis A, Dubée V, Sutterlin L, Atze H, Etheve-Quelquejeu M, Hugonnet JE, Arthur M. Tryptophan Fluorescence Quenching in β-Lactam-Interacting Proteins Is Modulated by the Structure of Intermediates and Final Products of the Acylation Reaction. ACS Infect Dis. 2019 Jul 12;5(7):1169-1176. doi: 10.1021/acsinfecdis.9b00023. Epub 2019 May 14. PMID: 31056908.
9. Chen J, Zhao L, Mao Y, Ye M, Guo Q, Zhang Y, Xu L, Zhang Z, Li B, Chu H. Clinical Efficacy and Adverse Effects of Antibiotics Used to Treat *Mycobacterium abscessus* Pulmonary Disease. Front Microbiol. 2019 Aug 23;10:1977. doi: 10.3389/fmicb.2019.01977. PMID: 31507579; PMCID: PMC6716072.
10. Buynak, J. D.; Al-Kharji, N. M. S. A.; Chai, W.; Nguyen, T. Q.; Alqurafi, M.; Rohde, K.; Gupta, R. C5-substituted carbapenem antibiotics, compositions containing such compounds, and methods of use in treatment of Mycobacterium tuberculosis and non-tubercular mycobacteria. US20180353476A1, 2018.
11. Gupta R, Al-Kharji N, Alquarafi M, Nguyen T, Chai W, Quan P, Malhotra R, Simcox B, Mortimer P, Brammer Basta L, Rohde K, Buynak J. Atypically modified carbapenem antibiotics display improved antimycobacterial activity in the absence of β-lactamase inhibitors. ACS Infectious Diseases 2021, 7 (8), 2425-2436. DOI: 10.1021/acsinfecdis.1c00185.
12. Majiduddin FK, Materon IC, Palzkill TG. Molecular analysis of beta-lactamase structure and function. Int J Med Microbiol. 2002 Jul;292(2):127-37. doi: 10.1078/1438-4221-00198. PMID: 12195735.
13. Zandi TA, Marshburn RL, Stateler PK, Brammer Basta LA. Phylogenetic and Biochemical Analyses of Mycobacterial l,d-Transpeptidases Reveal a Distinct Enzyme

Class That Is Preferentially Acylated by Meropenem. ACS Infect Dis. 2019 Dec 13;5(12):2047-2054. doi: 10.1021/acsinfecdis.9b00234. Epub 2019 Oct 14. PMID: 31597040; PMCID: PMC6910976.

14. Kuzmic P. Program DYNAFIT for the analysis of enzyme kinetic data: application to HIV proteinase. Anal Biochem. 1996 Jun 1;237(2):260-73. doi: 10.1006/abio.1996.0238. PMID: 8660575.
15. Kuzmic P. Dealing with uncertainty: Confidence intervals. http://www.biokin.com/courses/BKEB/pdf/lec07-h2.pdf (accessed on 2023-04-21).

Appendix 1

Term	Short for	Explanation/Background
Ldt	L, D-transpeptidase	Enzyme that forms 3→3 crosslinks
PBP	Penicillin binding protein	Enzyme that forms 4→3 crosslinks
Mtb	*Mycobacterium tuberculosis*	Mycobacteria responsible for TB
Ddt	D, D-transpeptidase	See also PBP
PG	Peptidoglycan layer	Essential layer outside a cell membrane essential for cell survival
TB	Tuberculosis	Mycobacterial infection caused by *Mtb*
Crosslink		Covalent bonds that connect the PG layer in bacterial cell walls
3→3 crosslinks		Predominant PG crosslink in mycobacteria
4→3 crosslinks		Predominant PG crosslink in most bacteria
β-lactams		Type of compound, inactivate PBPs, component of common antibiotics
carbapenem		Subclass of β-lactams that effectively inhibit Ldt function and includes meropenem, imipenem, and synthetic drugs **10a** and **10b**
MIC	Minimum inhibitory concentration	The lowest concentration of drug required to kill a bacterium; low values indicate a good drug
Mechanism		Way by which a reaction occurs
k_1 and k_2	Kinetic/rate constants	Indicate how quickly a reaction occurs
In vitro		Testing typically done in a test tube or petri dish